

Proceedings of the Institution of Mechanical Engineers, Part P: Journal of Sports Engineering and Technology

<http://pip.sagepub.com/>

Air flow around the point of an arrow

James L Park, Michael R Hodge, Salam Al-Mulla, Michael Sherry and John Sheridan

Proceedings of the Institution of Mechanical Engineers, Part P: Journal of Sports Engineering and Technology 2013 227:
64 originally published online 13 December 2011
DOI: 10.1177/1754337111430569

The online version of this article can be found at:
<http://pip.sagepub.com/content/227/1/64>

Published by:



<http://www.sagepublications.com>

On behalf of:



Institution of Mechanical Engineers

Additional services and information for *Proceedings of the Institution of Mechanical Engineers, Part P: Journal of Sports Engineering and Technology* can be found at:

Email Alerts: <http://pip.sagepub.com/cgi/alerts>

Subscriptions: <http://pip.sagepub.com/subscriptions>

Reprints: <http://www.sagepub.com/journalsReprints.nav>

Permissions: <http://www.sagepub.com/journalsPermissions.nav>

Citations: <http://pip.sagepub.com/content/227/1/64.refs.html>

>> Version of Record - Mar 7, 2013

OnlineFirst Version of Record - Dec 13, 2011

What is This?

Air flow around the point of an arrow

**James L Park, Michael R Hodge, Salam Al-Mulla,
Michael Sherry and John Sheridan**

Abstract

The aerodynamic drag of an arrow is of importance in relation to the arrow's drift in wind and to its down-range velocity. A significant contributor to that drag is the viscous drag from the arrow shaft, and consequently the nature of air flow over the arrow point and the location of the transition from laminar to turbulent flow are of interest.

In this paper the flow was investigated using a scale model in a water channel for two arrow point profiles and for circumferential gaps at the rear of the arrow point. The normal 'bullet point' was found to have laminar flow along the front of the shaft and transition at a Reynolds number of approximately 450,000, and that circumferential gaps did not affect the flow. The frequently used 'short bulge point' was found to have flow separation at the rear taper of the point and turbulent flow for the full length of the shaft, which would be expected to result in greater drag than for the bullet point or for a bulge point with less aggressive rear taper.

Keywords

Arrow, drag, turbulence, water channel, particle image velocimetry

Date received: 31 August 2011; accepted: 31 October 2011

Introduction

Major target archery competitions, such as the Olympic Games or World Championships, are generally conducted using outdoor venues exposed to wind. The distance used for these competitions is often 70 m, although in some cases distances as great as 90 m are used. The centre scoring ring on the target face at those distances has a radius of 61 mm, and in even a gentle breeze the drift of an arrow due to wind can easily exceed that.

The arrow aligns itself, on average, with the vector sum of its forward velocity and the wind velocity. The arrow's aerodynamic drag then has a lateral component due to that vector sum, and that results in lateral displacement (or 'wind drift'). The arrow's flexing and its longitudinal rotation as it aligns itself to that vector sum result in the angle of attack of the arrow point varying by a small amount during the arrow flight.

The archer (usually) tries to allow for this wind drift by aiming off from the centre of the target. An arrow with less drift for a given wind strength is of advantage in reducing the inevitable errors.

In a second major form of international archery competition, field archery, the archers are not told the distance to some of the targets (although they are within a given range, depending upon the target face

size) and the archers may have to shoot either up or down hills. A higher down-range arrow velocity is of advantage in minimising errors made by the archer in estimating the target distance and the allowance for slopes. A higher initial velocity (from using an arrow of lower mass) and reduced drag are hence both desirable. Consequently, understanding the component parts of the drag of an arrow is important.

A major proportion of the drag is due to the viscous drag of the arrow shaft. Airflow is initially laminar and then, a short distance along the shaft, transitions to turbulence. The drag coefficient for the arrow shaft changes significantly depending upon the position of the transition between the two flow types, as seen from equation 7-21 and figure 7.10 in Olsen.¹

Several shapes of arrow point are used in major competition. In some of these the maximum diameter of the point is the same as the arrow shaft diameter (referred to here as a 'bullet' point). For others,

Proc IMechE Part P:
J Sports Engineering and Technology
227(1) 64–69
© IMechE 2011
Reprints and permissions:
sagepub.co.uk/journalsPermissions.nav
DOI: 10.1177/1754337111430569
pip.sagepub.com



commonly known as ‘bulge points’, the point has a maximum diameter a little greater than the arrow shaft diameter and then tapers to the same diameter as the arrow shaft where they meet. Bulge points are used in order to ease the difficulty of withdrawing the arrow from the target and to minimise wear on the front portion of the arrow shaft when it enters the target. In some cases the arrow point or point insert includes circumferential grooves near where the point joins the arrow shaft to aid identification of the point or insert type and mass.

There appear to be no published papers covering the nature of this air flow over an arrow point. Liston² considered the drag of an arrow but assumed that the flow over the whole length of the arrow shaft was turbulent. Park³ has shown that the arrow can be expected to have an angle of attack as it leaves the bow of up to several degrees and, consequently, the nature of the air flow for small angles of attack is also of interest.

This paper considers the transition point from laminar to turbulent flow and the influence on the flow of the point profile and of circumferential grooves.

Method

Arrows in common use for outdoor target archery are usually constructed from carbon fibre composite material, often over a small diameter aluminium tube. They may be tapered to either the front or to both ends, although some types are not tapered. Diameters typically range from about 4.5 mm to 6 mm, depending upon the arrow type and size. The points used with these arrows often have a bulge, and are either made from stainless steel or tungsten, with the tungsten points having a shorter length and more severe rear slope in view of the significantly greater density of tungsten and hence the smaller volume required for a given arrow point mass. Low mass arrows, also usually constructed from carbon fibre composite material, are sometimes used for field archery, and typically have a constant shaft diameter of about 6–8 mm and use an arrow point with no bulge.

Typical arrow velocities range from approximately 55 m/s to 65 m/s for a recurve bow and from approximately 70 m/s to 100 m/s for a compound bow.

Flow around the point and front of a typical target archery arrow shaft was tested in water at a scale of 15.2:1 and with a water flow velocity of 0.456 m/s. The kinematic viscosity of water was 1.01×10^{-6} m²/s and that for air was 1.52×10^{-5} m²/s. A scale model of the arrow shaft was constructed using 76 mm diameter aluminium tube. Transition from laminar to turbulent flow was expected to occur at a Reynolds number of approximately 500,000 and hence at approximately 1.1 m along the shaft, so a shaft length of 2 m was used.

Scale models of both a typical short bulge point and a typical bullet point were machined from aluminium. In both cases the join between the point and the shaft

was smooth and with matching gradients at the join. The profiles of the actual points were as shown in Figure 1. A typical bullet point is shown at the bottom of Figure 1 and a short tungsten bulge point in the centre. As a comparison, a longer stainless steel bulge point is shown at the top. The maximum diameter of the actual short bulge point (not the scale model) was 5.3 mm, and it reduced to the diameter of 4.7 mm of the arrow shaft over a length of 4.5 mm. The alternative stainless steel point rear taper length was 19 mm. The difference in gradients of the rear slopes of the tungsten and stainless steel points is obvious in Figure 1. The profiles of the model bulge and bullet points are shown in Figure 2.

The model arrow was supported in the water channel from the rear such that its angle of attack could be varied from 0° to 3°. The water flow around the point and shaft was examined using a UV-sensitive dye and using particle image velocimetry. The model arrow, with bulge point, is shown in the water channel in Figure 3. The cases considered are listed in Table 1.

UV dye tests

A UV sensitive dye (fluorescein) was mixed with honey, which adhered to the test models. Flow around the bullet point with an angle of attack of 0° was laminar and remained so across the boundary onto the arrow shaft. Transition occurred at a distance along the arrow of 1.0 m, corresponding to a Reynolds number of 450,000. Figure 4 shows laminar flow over the bullet point and along the shaft. Figure 5 shows laminar flow along the shaft with the bullet point and transition to turbulent flow.

As the angle of attack was increased there was circumferential flow around the shaft and the transition distance moved forward on the pressure edge and back on the suction edge by approximately 0.1 m in each case at an angle of attack of 3°. The flow remained

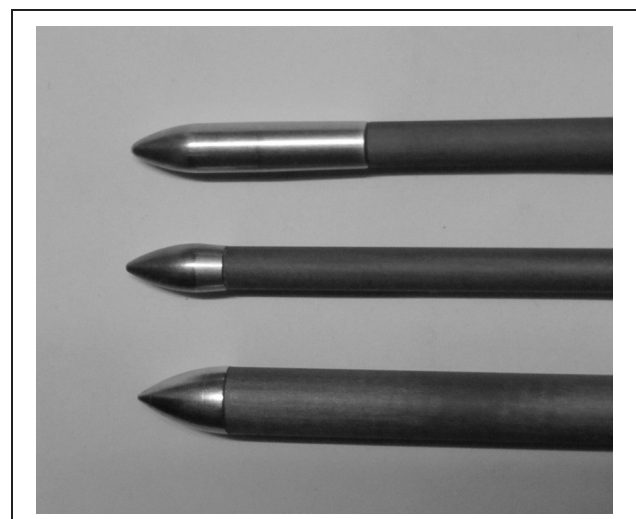


Figure 1. Arrow point profiles (of the actual arrows).

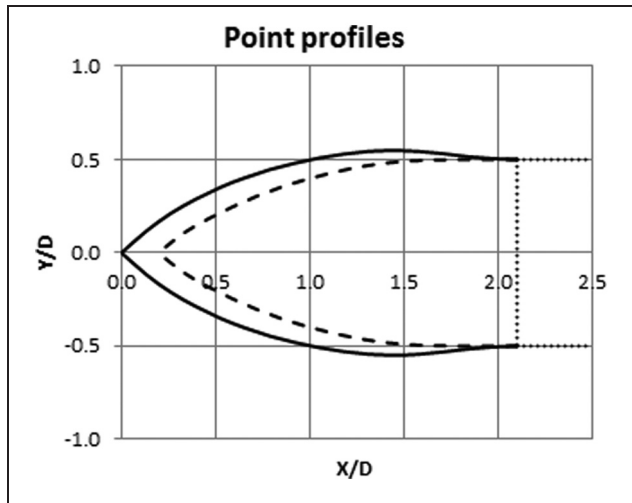


Figure 2. Schematic showing a 2D profile of the arrow points tested. Length and height dimensions are non-dimensionalised by the arrow shaft diameter, D, and referenced from the front of the arrow.



Figure 3. The model arrow in the water channel.

laminar around the point and across the joint to the arrow shaft. The average transition distance remained around 1.0 m.

Flow around the bulge point separated slightly downstream of the maximum bulge radius, as can be seen in Figure 6. Dye placed on the shaft just to the rear of where the point joins the arrow shaft did show reverse flow on the rear taper of the point, indicating recirculation at that position. The water velocity was

Table I. List of test cases.

Point type	Circumferential gap	Angle of attack($^{\circ}$)	Notes
Bullet	No	0, 1, 2, 3	Tests using dye, 0.456 m/s
Bullet	Yes	0	Test using dye, 0.456 m/s
Bulge	No	0, 1, 2, 3	Tests using dye and PIV, 0.092–0.456 m/s

PIV: particle image velocimetry.

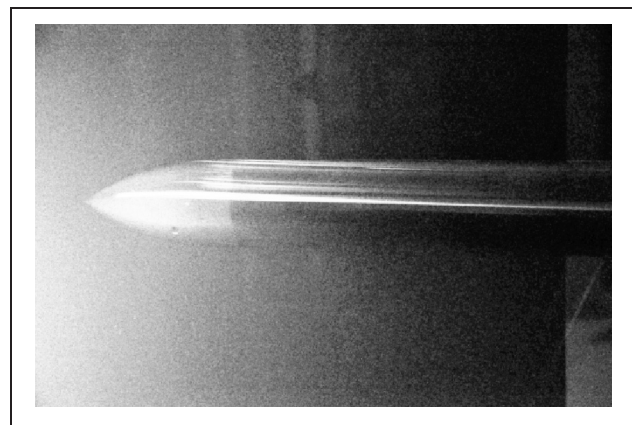


Figure 4. Laminar flow over the bullet point at an angle of attack of 1° .



Figure 5. Laminar flow and transition with the bullet point.

lowered until separation ceased at a velocity of 0.092 m/s. At a velocity of 0.321 m/s there was separation at the decreased radius but immediate reattachment and laminar flow along the shaft. At 0.365 m/s there was turbulent flow over the whole test length from the rear end of the recirculation area. Consequently, turbulent flow can be expected for all typical velocities for arrows shot using compound bows and for most arrows shot using recurve bows.

Flow was certainly turbulent at the start of the taper on the trailing edge of the bulge point for all angles of attack at a water velocity of 0.456 m/s. The transition

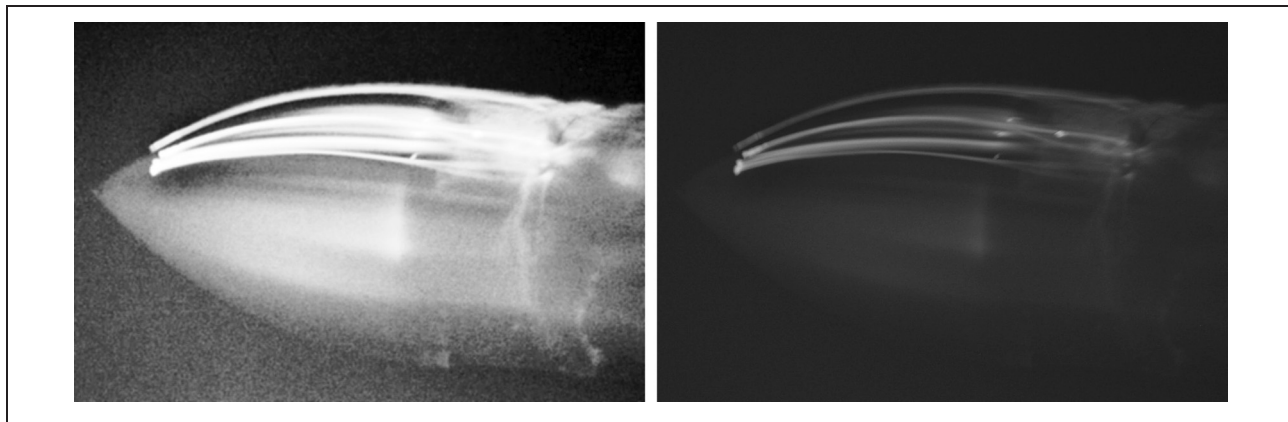


Figure 6. Separation at the trailing taper of the bulge point.

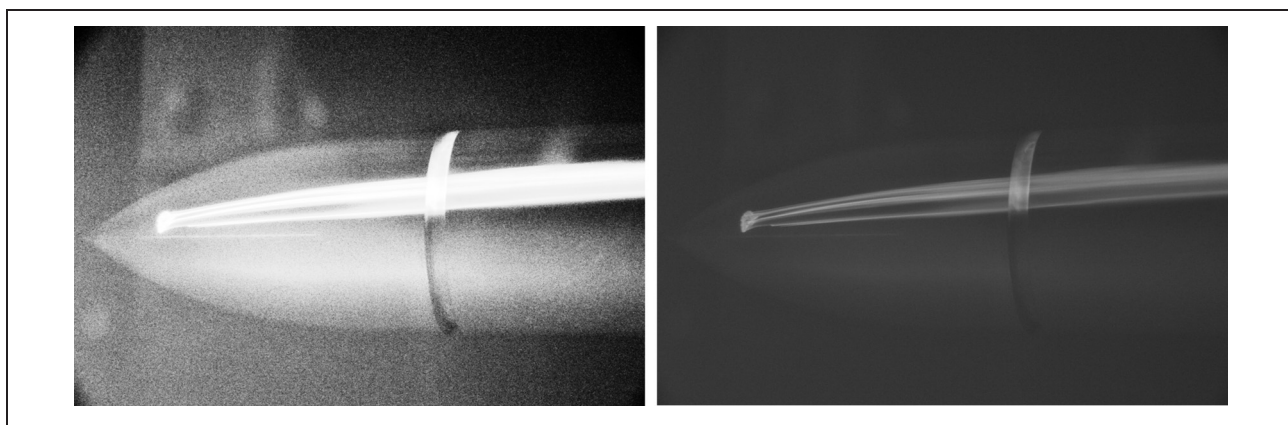


Figure 7. Flow over a circumferential gap between the point and the shaft with the bullet point.

point moved back along the shaft by approximately 5 mm on the leading edge for an angle of attack of 3°.

A small amount of flow-induced vibration of the arrow shaft was observed for the bulge point, but not for the bullet point. This was consistent with the nature of flow over the two point profiles, with the bulge point having vortices formed and shed from the recirculation region.

The bullet point was moved forward in the arrow shaft by distances of up to 10 mm to create a circumferential gap with a depth of 3.6 mm between the point and the shaft in order to study the impact on the flow. Flow remained laminar over the gap and along the shaft, with a similar transition point to the case where there was no gap, as shown in Figure 7. Within the gap there was minimal flow (the dye in the gap moved very slowly around the circumference of the shaft).

Particle image velocimetry results

In view of the recirculation region seen when testing the bulge point, particle image velocimetry (PIV) measurements were made for that arrow point for angles of attack from 0° to 3°.

PIV is a non-intrusive optical experimental technique utilising the reflective properties of neutrally buoyant

seed particles to capture fluid particle displacements over a known time interval in a specific region of interest. The free stream flow is seeded with particles (hollow glass spheres of diameter 10 µm) of neutral density which follow the fluid accurately. A pulsed laser (continuum Minilite, wave length 532 nm, energy per pulse 25 mJ) was formed into a sheet of thickness ≈2 mm by a mirror and optical lens set. The laser sheet illuminated the region of interest behind the arrow point bulge. One thousand pairs of digital images were captured with a CCD camera with a known time delay. In-house validated PIV cross correlation software was used to produce displacement, velocity and vorticity fields.⁴ The data were acquired at a uniform sample rate of 1 Hz, so the samples can be considered uncorrelated.

A velocity vector plot constructed from the 1000 image pairs for the 0° angle of attack case is shown in Figure 8. Only the top half of the arrow bulge is shown as the flow was symmetrical. The free stream flow was from left to right and flow uniformity was evident from $Y > 1.2D$. Closer to the arrow surface (i.e. $Y < 1.2D$), the flow deviated from this uniformity. The flow separated from the arrow surface at approximately $X = 1.61D$, where the origin is taken as the front of the arrow's point. The separation point was clearly evident

in the raw PIV images by an accumulation of seeding particles. A free shear layer formed between the low velocity recirculating fluid close to the arrow surface and the free stream flow. The free shear layer impinged on the arrow surface downstream, creating a separation region, as depicted by the contour line encapsulating the black region in Figure 8. Vorticity was created on the front surface of the arrow and is clearly evident within the free shear layer and the recirculation region and promotes turbulent flow along the entire arrow shaft. Kelvin Helmholtz vortices (seen in the instantaneous images from the PIV) formed in the free shear layer and advected downstream, creating time-varying loading on the arrow shaft (possibly leading to the vibration of the arrow shaft, as noted above during the dye testing for all angles of attack). The dimensions of the recirculation region were of primary interest in the PIV measurement results.

A velocity vector plot for the 2° angle of attack case is shown in Figure 9. Again the free stream flow was from left to right. A distinct asymmetry formed between the upper and lower recirculation regions due to the angle of attack and the asymmetry in the resulting pressure distribution. The increased surface curvature on the upper surface of the arrow head encouraged an adverse pressure gradient to form earlier, and hence

separation occurred earlier, compared to the 0° case. With a reduction in the surface curvature on the lower arrow surface, the separation point moved slightly downstream. This asymmetry grew with angle of attack, as expected. The growth of the asymmetry can be seen in Figure 10. The asymmetry of the recirculation region behind the bulge created a three dimensional flow field associated with the separation region which can be expected to affect the stability of flight.

Discussion

Flow along the arrow with the bullet point and for small angles of attack can be accurately modelled assuming transition from laminar to turbulent flow at a Reynolds number of approximately 450,000. For example, for a typical competition arrow with bullet point travelling at a velocity of 85 m/s, transition can be expected to occur at approximately 81 mm along the arrow shaft.

Flow along an arrow with a bulge point is more complex. With the short bulge point and at the usual range of velocities for both recurve and compound bows one can expect to have separation where the arrow point diameter reduces, even for zero angle of attack, and that the flow will remain turbulent from the end of the recirculation zone along the full length of the arrow shaft, corresponding to a transition Reynolds number of 90,000, as measured from the front of the point. This can be expected to increase the arrow's drag compared to a point profile where separation was avoided. The flow did not separate for an equivalent arrow velocity of approximately 56 m/s, although that is a lower velocity than would generally be expected for either a recurve or a compound bow.

The alternative (and lower cost) long bulge point has a much gentler rear taper (by a factor of approximately four). While this was not tested, it can be expected to be much less likely to provoke separation, and hence is likely to have lower drag. A transition Reynolds number of 450,000 would be appropriate. It is consequently a better choice for minimising wind drift of an arrow.

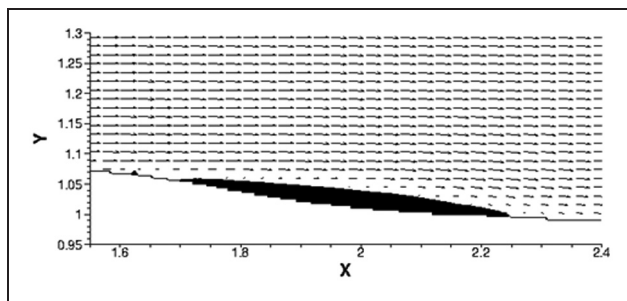


Figure 8. Velocity vector plot of the flow behind the arrow point bulge at a 0° angle of attack. The vector magnitude is reduced by two and every eighth vector in the x -direction and every fourth vector in the y -direction is shown for clarity. The black region indicates the region of negative axial velocity.

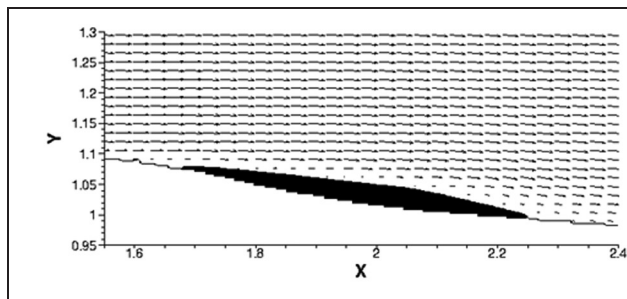
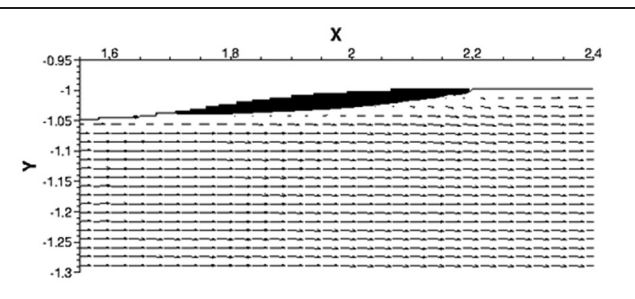


Figure 9. Velocity vector plots of the flow behind the arrow head bulge at 2° angle of attack. The top figure depicts the upper recirculation region and the bottom figure depicts the lower separation region. The vector magnitude was reduced by two and every eighth vector in the x -direction and every fourth vector in the y -direction is shown for clarity. The black region indicates the region of negative axial velocity.



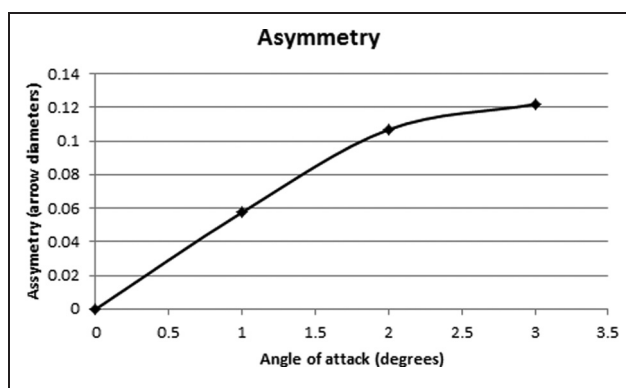


Figure 10. Recirculation region asymmetry for the bulge arrow point.

The importance of the nature of the flow around the arrow point can be considered using a simple example. Consider the wind drift of an arrow with an average diameter of 5.20 mm, of length 0.71 m and mass 25.03 gm. Using the method described by Park,⁵ the calculated wind drift for a distance of 70 m, an initial arrow velocity of 84.1 m/s and with a side wind of 3 m/s is 156 mm when a bullet point is used. If a short bulge point is used the wind drift increases to 161 mm. The difference corresponds to approximately a full arrow diameter, which is certainly of interest.

Conclusions

Air flow around a bullet point can be expected to be laminar, with a well-defined transition point along the

shaft to turbulent flow at a Reynolds number of 450,000.

The rear taper angle of typical short bulge points is likely to lead to flow separation at the rear taper, turbulent flow along the full length of the arrow and, consequently, to increased drag and wind drift.

The circumferential grooves used on some arrow points (for identification) can be expected to have little influence on the air flow or drag.

Funding

This research received no specific grant from any funding agency in the public, commercial, or not-for-profit sectors.

References

1. Olsen R M. *Engineering fluid mechanics*. Scranton, PA: International Textbook Company, 1967.
2. Liston T L. *Physical laws of archery*. San Jose, CA: Liston & Associates, 1991.
3. Park J L. The behaviour of an arrow shot from a compound archery bow. *Proc IMechE Part P: J Sports Engineering and Technology* 2011; 225(1): 8–21.
4. Fouras A, Lo Jacino D and Hourigan K. Target-free stereo PIV: a novel technique with inherent error estimation and improved accuracy. *Experiments in Fluids* 2008; 44(2): 317–329.
5. Park, J L. Minimizing wind drift of an arrow. *Proc IMechE Part P: J Sports Engineering and Technology*. Epub ahead of print 30 September 2011. DOI: 10.1177/1754337111418876.